MECHANIKA
CZASOPISMO TECHNICZNE
TECHNICAL TRANSACTIONS
MECHANICS
WYDAWNICTWO POLITECHNIKI KRAKOWSKIEJ
4-M/2010
ZESZYT 20
ROK 107
ISSUE 20
YEAR 107

GRZEGORZ WIDŁAK, ANDRZEJ P. ZIELIŃSKI*

CYCLIC STEADY STATES OF A THICK-WALLED REACTOR WITH STRESS CONCENTRATORS

CYKLICZNE STANY USTALONE W GRUBOŚCIENNYM REAKTORZE Z KONCENTRATORAMI NAPRĘŻEŃ

Abstract

The paper deals with elastic-plastic stress states in vicinity of a radial cross-bore in a thick-walled reactor loaded by variable internal pressure and a temperature gradient. In the description of material, the linear Prager model of hardening has been applied. The mechanism of development of reverse plastification in each load cycle has been observed. The termal effect is presented on an example of the steady stress states. The transient states (starting and closing work periods of the reactor) have been investigated in the PhD thesis of the first author

Keywords: *thick-walled reactor, radial cross-bore, shakedown, thermal effects, finite element method*

Streszczenie

W artykule badano sprężysto-plastyczne stany naprężeń w pobliżu otworu grobościennego reaktora obciążonego zmiennym ciśnieniem wewnętrznym i różnicą temperatur. W opisie materiału stosowano liniowy model wzmocnienia Pragera. Obserwowano mechanizm rozwoju przeciwzwrotnego uplastycznienia występujący przy każdym cyklu obciążenia. Efekty termiczne pokazano na przykładzie stanów ustalonych. Stany nieustalone (rozruch i wygaszanie reaktora) były badane w ramach rozprawy doktorskiej pierwszego autora.

Słowa kluczowe: *reaktor grubościenny, otwór promienny, przystosowanie plastyczne, efekty termiczne, metoda elementów skończonych*

* Dr inż. Grzegorz Widłak, Prof. dr hab. inż. Andrzej P. Zieliński, Instytut Konstrukcji Maszyn, Wydział Mechaniczny, Politechnika Krakowska.

1. Introduction

High-pressure, thick-walled cylindrical vessels, which are used in the petrochemical and other process industry are usually subject to cyclic mechanical and thermal loads. Such vessels very often have small radial holes in their walls, which are necessary for media transmission and attachment of instrumentation. These holes are strong stress concentration sources and in their vicinity plastic effects can often occur. Therefore, it is essential to design the vessels against cyclic plasticity failure mechanisms, which can result in development of cracks dangerous for the whole structure. The cracks of this kind were observed in one of polyethylene reactors in the petroleum refinery in Poland [1, 2]. They appeared near a small hole for discharging the reactor from the final product (Fig. 1). The purpose of the present work is, therefore, to examine closely and comprehensively this important industrial problem with respect to local plasticity effects during cyclic operating of the reactor.

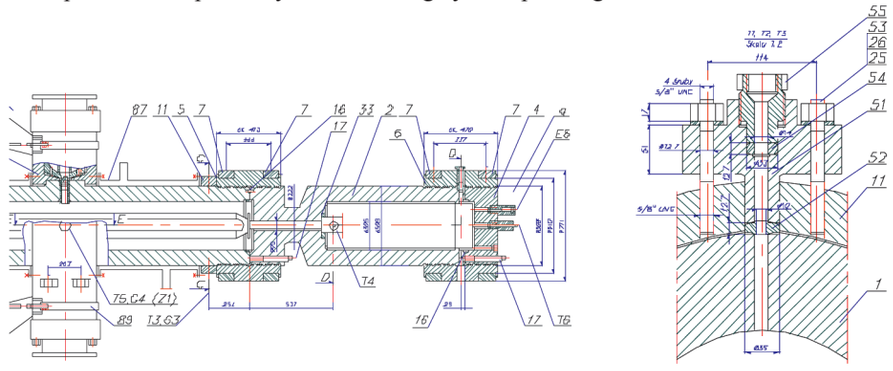

a) b)

Fig. 1. Reactor used in the petroleum refinery: a) general view, b) object of interest – radial hole and its vicinity

Rys. 1. Reaktor stosowany w rafinerii ropy naftowej: a) widok ogólny, b) okolice promieniowego otworu – przedmiot badań

2. Cyclic response of thick-walled reactor subject to pressure load

In the present section a mechanism of development of reverse plastifications is illustrated. A simple assessment of the linear kinematic hardening rule is also presented in the context of the ratchetting evaluation.

2.1. Material model

The rate-independent plasticity model used in this study is assumed to exhibit kinematic hardening with the Huber – von Mises yield condition [3]. Therefore, the equivalent stress can be defined as

$$\sigma_e = \left(\frac{3}{2} (\mathbf{S} - \mathbf{a}) : (\mathbf{S} - \mathbf{a}) \right)^{1/2} \tag{1}$$

where **S** is the deviatoric stress tensor and **a** denotes the back stress deviator, representing current center of the yield surface. The yield function

$$f = \sigma_e - Y_0 \tag{2}$$

gives yield condition $f = 0$, which must hold throughout the plastic response. The size of the yield surface is denoted by Y_0, which remains constant in kinematic hardening models. There are many formulations of coupled kinematic models [4]. Prager proposed [5] the simplest possible form of evolution of the yield surface during plastic straining by linear translation in the stress space:

$$\dot{\mathbf{a}} = \frac{2}{3} C \dot{\boldsymbol{\varepsilon}}^{\mathbf{pl}} \tag{3}$$

This model is very popular in engineering computations, because it needs only one plastic parameter C. Despite the fact that this model could reasonably represent the shape of some monotonic stress-strain curves, it fails to produce ratchetting in uniaxial tests. Moreover, rapid prediction of shakedown in the initial cycles of multiaxial loading does not match experimental results. More appropriate models were investigated in [6]. Nevertheless, in the first approach to the problem, it seems to be reasonable to use this simple model in order to demonstrate mechanisms responsible for the development of cyclic plasticity. In further calculations the values of Y_0 = 275 MPa and C = 2000 MPa were assumed.

2.2. FE model

In reactors, the pressure load and thermal gradients usually have cyclic character, therefore it is essential to develop a FEM model (Ansys), which is appropriate for accurate and effective cyclic plasticity simulations [7]. Estimation and investigation of the robust integration algorithm of constitutive equations, which is herein utilized, can be found in [8].

It has been assumed that the investigated reactor has the following dimensions (compare Fig. 2): internal radius a =150 mm, external radius is defined by ratio a/b = 0,7 and radial hole diameter ratio is d/a = 0,05. The radial crosshole configuration has two planes of symmetry, so only a quarter-models are required (see Fig. 3). The x-R plane has the following symmetry conditions

$$\begin{cases} u_\theta = 0 \\ \tau_{\theta R} = 0 \\ \tau_{\theta x} = 0 \end{cases} \tag{4}$$

and the $x - \theta$ plane

$$\begin{cases} u_x = 0 \\ \tau_{xR} = 0 \\ \tau_{x\theta} = 0 \end{cases} \tag{5}$$

where u_θ, u_x are corresponding direct displacements and $\tau_{\theta R}$, $\tau_{\theta x}$, τ_{xR}, $\tau_{x\theta}$ represent shear stresses.

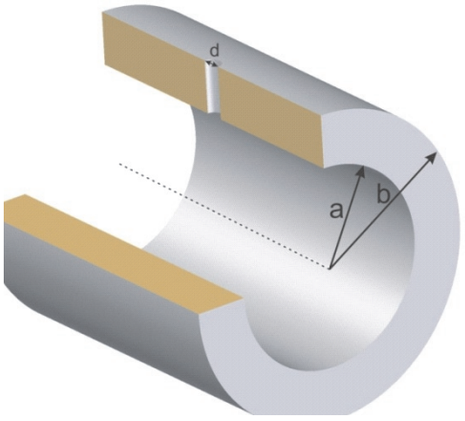

Fig. 2. General view of investigated reactor model

Rys. 2. Ogólny widok modelu badanego reaktora

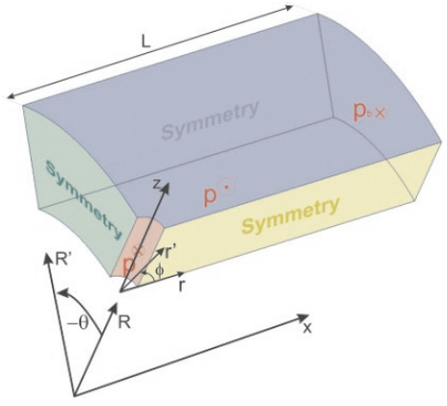

Fig. 3. Reduced computational model and boundary conditions; global and local coordinate systems

Rys. 3. Model obliczeniowy i jego warunki brzegowe; globalny i lokalny układ współrzędnych

Dimensions of the segment are suitably chosen so as not to disturb the local stress field. A pressure load p is applied on the internal surface of the main bore as well as on the radial hole surface. The closed-end boundary condition is defined by application of uniform axial tension at the end of the cylinder

$$p_b = p\frac{(a/b)^2}{1-(a/b)^2} \tag{6}$$

The presented segment is discretized with 13200 higher-order finite elements. Every element is defined by 20 nodes having three translational degrees of freedom per node. A specific value of the pressure load, loading manner as well as thermal boundary specification are given in the successive sections, which describe particular analyses.

2.3. Mechanism of development of reverse plastification

Radial holes in the thick-walled vessel structure, have negligible influence on reduction of the global load-carrying capacity. Nevertheless, they are strong stress concentration sources, causing significant decrease of elastic limit loads and rapid plastification near the hole [6].

In order to demonstrate characteristic mechanism which is responsible for the development of cyclic plasticity, loading and unloading process has been simulated. For the given pressure values up to $3p_0$ (p_0 = 32 MPa – is the reactor elastic capacity), the material effort state and redistribution of the principal stresses are observed. The maximum effort point is identified

in the subsequent stages. In Fig. 4 and Fig. 5 a position of this point is presented. It is located on the edge between the radial hole surface and the x-R symmetry plane. Therefore, dimensionless shift $\zeta = z / c$ uniquely defines its location. The axial local coordinate is herein denoted by z, whereas c is the thickness of reactor wall.

With the increase of pressure, a proportional decrease of the minor stresses is observed. The minor stress direction coincides with the radial local coordinate. A slight decrease, in order to fulfill the consistency condition, of the major (hoop direction) and middle (axial direction) stresses is noticed. Such a tendency is observed in all the subsequent maximum effort points, in which the principal directions are illustrated in the figures below.

An essential redistribution of principal directions is noticed during the unloading process (Fig. 5). Just below the relief pressure $p/p_0 = 2$, a characteristic stress state occurs, in which the initially positive major (hoop) stress changes to be compressive and its value is equal in this moment to the axial stress magnitude. Therefore, in the plane determined by the axial direction and the tangent to the circumferential direction in this point, the shear vanish and the normal stresses in all directions are the same (local hydrostatic state).

Furthermore, with the progressive relief, a proportional decrease of compression in the radial principal direction is observed. Eventually, it reaches a zero value and the radial direction could be considered as a major principal direction. A strong compression of the plastified zone, occurring in the hoop direction, contributes to the considerable change of the order of principal stresses. The final stress state, results in reverse plastification and the active process causes further shift of the maximum effort point. Incompressibility of the plastic flow produces also in this case considerable enlargement of compression in the axial direction.

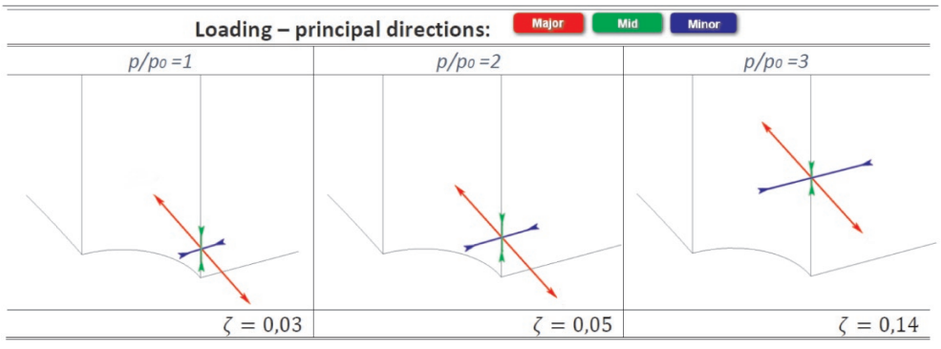

Fig. 4. Stresses in principal direction at the maximum effort point ($p_0 = 32$ MPa), $\zeta = z / c$, z – reactor thickness

Rys. 4. Naprężenie główne w punkcie maksymalnego natężenia ($p_0 = 32$ MPa) – obciążenie, $\zeta = z / c$, z – grubość reaktora

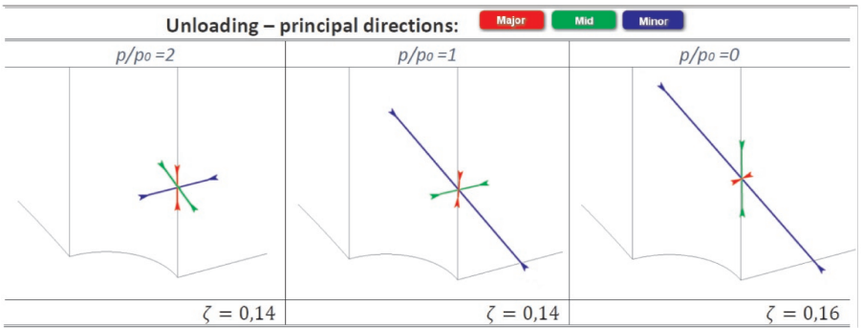

Fig. 5. Stresses in principal direction at the maximum effort point (p_o = 32 MPa), $\zeta = z / c$, z – reactor thickness

Rys. 5. Naprężenia główne w punkcie maksymalnego wytężenia (p_o = 32 MPa) – odciążenie, $\zeta = z / c$, z – grubość reaktora

2.4. Inadaptation range

When reactor loads exceed elastic shakedown limit, phenomenon of cyclic plasticity occurs, which is a cause of fatigue failure in very-low-cycle and low-cycle regimes. In addition to alternating plasticity, a ratchetting response is often present, accounting for acceleration of fatigue damage or acting as a failure mechanism itself. Although, plastic strains developed in the first cycle are relatively low, they can be accumulated in a predominant direction during subsequent cycles. The accumulation of plastic strains is one aspect of cyclic plasticity. The other, appearing in the fatigue damage form, is characterized by micro- and macro-crack propagation process and final fracture. However, there is a strong interaction between the damage processes. Crack initiation and propagation are strongly affected by the accumulated plastic strains.

Operating in an inadaptation range is admitted by some design codes. Moreover, when the number of cycles is so low that the fatigue damage is prevented, as it is in the case of reactors, emphasis should be put on check of progressive deformation. This requires application of appropriate models of ratchetting, which can result in failure itself.

In the pressure vessel with a hole, translation of the point of max. effort (Fig. 4, Fig. 5) fades with the cycling and this point settles in the initial location corresponding to the first loading. In the case of modelling of the ratchetting mode, magnitude of plastic strains change and progressive deformation is observed in the surrounding regions, as it has been demonstrated in [6]. In the following, plastic strain components are presented for the maximum effort point, as a function of the number of cycles (Fig. 6). For the Prager hardening model, there are no significant changes in the plastic strain history. After initial, relatively large plastification, a reverse plasticity is observed due to strong compressive effects after unloading (1st cycle). A slight difference between magnitudes of plastic strain increments during loading and unloading is noticeable only for the first three cycles. Further, an integral of every component of plastic strain tensor is practically equal to zero over each individual cycle. Therefore, the linear Prager model should not be used for representation of ratchetting in this specific structre.

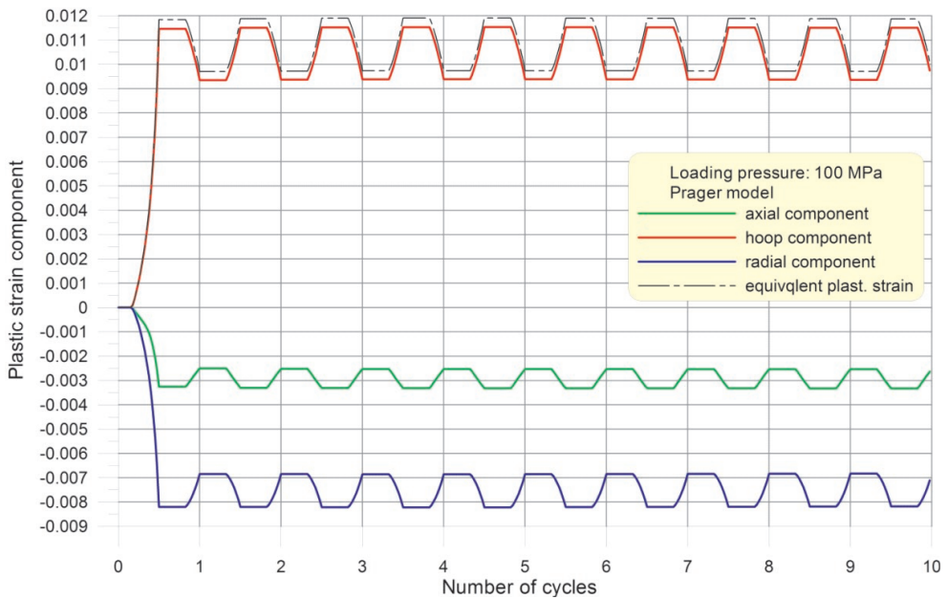

Fig. 6. Plastic strains (local hole coordinates) induced by 100 MPa pressure loading – Prager hardening rule (a/b = 0,7; d/a = 0,01)

Rys. 6. Odkształcenia plastyczne (współrzędne lokalne otworu) wywołane tętniącym ciśnieniem 100 MPa – model wzmocnienia Pragera (a/b = 0,7; d/a = 0,01)

As it has been noticed above, the case with linear hardening model shows slight increments of plastic strains, which is rather caused by a redistribution effect and expires with the further cycling (Fig. 7).

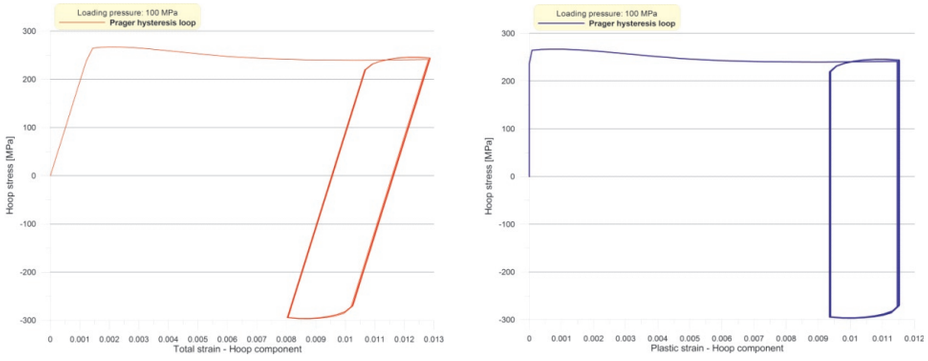

Fig. 7. Hysteresis loop – Prager hardening rule

Rys. 7. Pętla histerezy – model wzmocnienia Pragera

3. Influence of thermal gradients at steady states

Up to now only the mechanical loading (pressure) has been considered. However, the high pressure reactors are usually subject to internal pressure and increased temperatures [9]. In the present section, the steady thermal effects are taken into account. The thermal gradient causes development of thermal stresses, moreover, the high temperatures can significantly change the material properties. The study concerns examination of reactors subjected to different pressure and thermal load relations during steady states of the loading-unloading cyclic process.

In order to evaluate temperatures in the reactor model, which is subjected to stabilized conditions, the well-known homogeneous equation of steady state heat transfer is utilized. Once the temperature field is known, resulting thermal strains and stresses are calculated [10]. For detailed investigation of the thermal effects, different combinations of pressure loads and associated steady temperature states have been chosen. The mechanical loadings are applied in the form of pressure which takes values: 60 MPa, 80 MPa and 100 MPa. On the internal reactor surfaces (Fig. 8) the convection boundary conditions are established with the convection coefficient $h_i = 2000\frac{\mathrm{W}}{\mathrm{m^2K}}$. Internal temperatures take values from $T_1 = 50°\mathrm{C}$ to $T_6 = 300°\mathrm{C}$ each $\Delta T = 50°\mathrm{C}$. The external reactor surface has the ambient boundary conditions with the convection coefficient $h_0 = 20\frac{\mathrm{W}}{\mathrm{m^2K}}$ and temperature $T_0 = 20°\mathrm{C}$.

A material model used in calculations corresponds to a typical boiler steel DIN13Cr-Mo44. The yield stress for this steel is $Y_{020} = 300\,\mathrm{MPa}$ for the temperature $T_0 = 20°\mathrm{C}$ and decreases to $Y_{0300} = 235\,\mathrm{MPa}$ in the temperature $T_{\max} = 300°\mathrm{C}$.

The first analysis concerns determination of temperature distribution with the specified boundary conditions. With the above assumed values of the convection coefficients, there are no significant thermal gradients in the steady state. For example, in the case of processed medium temperature $T_i = 300°\mathrm{C}$ and ambient temperature $T_0 = 20°\mathrm{C}$ the difference of internal and external temperatures of the vessel is equal $\Delta t = 11,2°\mathrm{C}$ (Fig. 9).

In the case of steady thermal effects different distributions of the stress and strain states in the vessel result mainly from the pressure changes. Presence of strong concentration causes that even for the lowest pressure the local plastic strain occurs. The pressure increase results in regular effort variation up to the highest analyzed temperatures in which a considerable yield stress reduction is observed and a significant shifting of the maximum effort point in the analyzed structure. The largest load configuration results in plastic strains which have a global range (Fig. 10).

A difference of the local equivalent plastic strains between the loaded and unloaded states

$$\Delta\varepsilon_{eq}^{pl\max} = \varepsilon_{eq}^{pl\,load} - \varepsilon_{eq}^{pl\,unload} \tag{7}$$

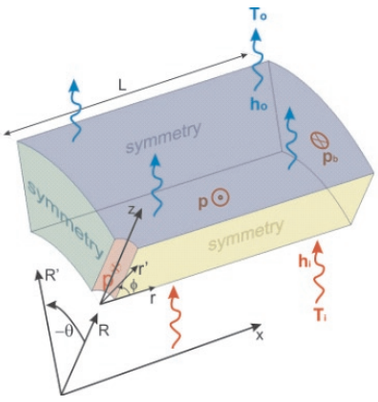

Fig. 8. A computational model – thermal boundary conditions

Rys. 8. Model obliczeniowy – termiczne warunki brzegowe

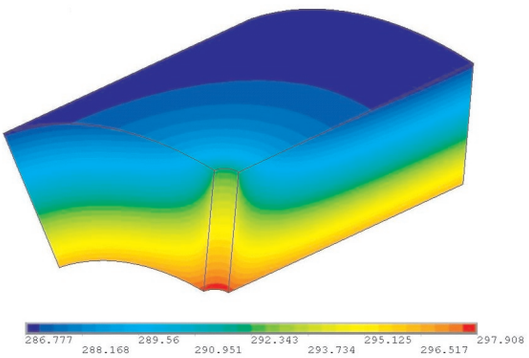

Fig. 9. Steady state temperature distribution (T_i = 300°C, T_0 = 20°C; t_{min} = 287°C, t_{max} = 298°C)

Rys. 9. Ustalony stan rozkładu temperatury (T_i = 300°C, T_0 = 20°C; t_{min} = 287°C, t_{max} = 298°C)

has been chosen as a measure of reverse plastification of the structure. This difference increases with increasing pressure but almost does not change with temperatures. Only the highest internal temperature causes its considerable reduction because of strong growth of the plastic strain zone in the vicinity of the hole, which results in decrease of compressive effects after unloading (Fig. 11).

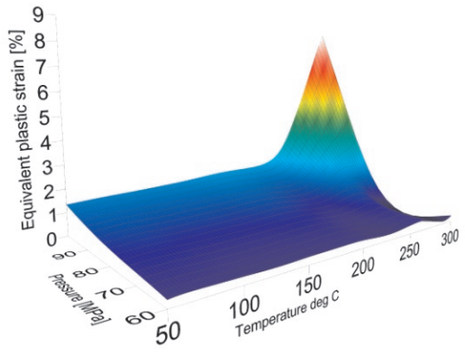

Fig. 10. Equivalent plastic strains after loading

Rys. 10. Zastępcze odkształcenie plastyczne po obciążeniu

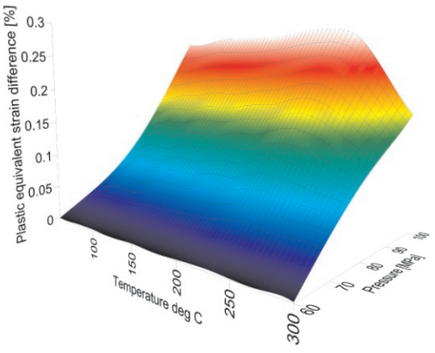

Fig. 11. Equivalent plastic strain difference (loading – unloading)

Rys. 11. Różnica odkształceń plastycznych (obciążenie – odciążenie)

4. Conclusions

The investigation of material models which are intended to represent cyclic plasticity (the Armstrong-Frederick and Chaboche models) proved [6] that the ratchetting rate in the reactor structure is significant at the initial process stage and further is kept constant, which eventually leads to the failure due to incremental plastic collapse. The constitutive model considered here (Prager hardening rule) is not intended to define cyclic plasticity. A plastic modulus C (Eqn (3)), which is the same for loading and unloading (no effect of mean stress) results, therefore, in the stress cycles, which form a closed hysteresis loop.

The small thermal effects noted above change to large values in starting and closing work periods of reactors (strongly unsteady states). These effects and their influence on local elastic-plastic response have been investigated in detail and are presented in [6].

References

[1] Ryś J., *Strength analysis in the region of a hole in high pressure vessel,* Proceedings of the 8th International Research Expert Conference "Trends in the Development of Machinery and Associated Technology TMT", Neum, 2004.

[2] Zieliński A.P., Łaczek S., Ryś J. *Optimization of Thick-Walled High-Pressure Vessels with Holes with Respect to Ductile Fracture*, Proceedings of the 6th World Congress of Structural and Multidisciplinary Optimization, Rio de Janeiro 2005.

[3] Życzkowski M., *Combined Loadings in the Theory of Plasticity*, PWN, Warszawa 1981.

[4] Chaboche J.L., *Time-independent constitutive theories for cyclic plasticity*, International Journal of Plasticity, 2, 1985.

[5] Prager W., *A new method of analyzing stresses and strains in work hardening plastic solids*, Journal of Applied Mechanics, 23, 1956.

[6] Widłak G., *Local shakedown analysis of a thick-walled reactor subject to mechanical and thermal loads.*, PhD thesis supervised by A.P. Zieliński, Cracow University of Technology, Cracow 2010.

[7] Zieliński A.P., Widłak G., *Local shakedown analysis in regions of holes in high pressure vessels,* Proceedings of the IX International Conference on Computational Plasticity, COMPLAS IX, Barcelona, 2007.

[8] Widłak G., *Radial return method applied in thick-walled cylinder analysis*, Journal of Theoretical and Applied Mechanics, 48, 2010.

[9] Camilleri D., Mackenzie D., *Shakedown of a thick cylinder with a radial crosshole*, ASME Pressure Vessels and Piping Division, 2006.

[10] Widłak G., Zieliński A.P., *Local shakedown analysis of reactors subject to pressure and thermal loads,* Proceedings of the 8th World Congress on Computational Mechanics, Venice 2008.